Acetate ion addition to and exchange in (1,5-cyclooctadiene)rhodium(i) acetate: relevance for the coagulation of carboxylic acid-functionalized shells of core-crosslinked micelle latexes

Ambra Maria Fiore, Valentina Petrelli, Christophe Fliedel, Eric Manoury, Piero Mastrorilli, Rinaldo Poli

ARTICLE

Acetate Ion Addition to and Exchange in (1,5-cyclooctadiene)-rhodium(I) Acetate: Relevance for the Coagulation of Carboxylic Acid-Functionalized Shells of Core-crosslinked Micelle Latexes

Received 00th January 20xx,
Accepted 00th January 20xx

DOI: 10.1039/x0xx00000x

Ambra Maria Fiore,[a,b] Valentina Petrelli,[b] Christophe Fliedel,[c] Eric Manoury,[c] Piero Mastrorilli*,[b] Rinaldo Poli*[c,d]

The solution behavior of complex $[Rh(COD)(\mu\text{-}OAc)]_2$ in the absence and presence of PPN^+OAc^- in dichloromethane has been investigated in detail by multinuclear NMR spectroscopy. Without additional acetate ions, the compound shows dynamic behavior at room temperature, consistent with an inversion of its C_{2v} structure. Addition of PPN^+OAc^- reveals an equilibrated generation of $[Rh(COD)(OAc)_2]^-$. Rapid exchange is observed at room temperature between the neutral dimer and the anionic mononuclear complex , as well as between the anionic complex and free acetate. Lowering the temperature to 213 K freezes the exchange between the two Rh complexes, but fast exchange between the anionic Rh complex and free acetate maintains coalesced Me (^1H and ^{13}C) and COO (^{13}C) NMR resonances. DFT calculations support the experimental data and lean in favour of a dissociative mechanism for the acetate exchange in $[Rh(COD)(OAc)_2]^-$. The acetate ligands in complex $[Rh(COD)(\mu\text{-}OAc)]_2$ are also exchanged in a biphasic (water/organic) system with the methacrylic acid (MAA) functions of hydrosoluble $[MMA_{0.5}\text{-}co\text{-}PEOMA_{0.5}]_{30}$ copolymer chains (PEOMA = poly(ethylene oxide) methyl ether methacrylate), resulting in transfer of the Rh complex to the aqueous phase. Exchange with the MAA functions in the same polymer equally takes place for the chloride ligands of $[Rh(COD)(\mu\text{-}Cl)]_2$. The latter phenomenon rationalizes the coagulation of a core-crosslinked micelle (CCM) latex, where MMA functions are present on the hydrophilic CCM shell, when a dichloromethane solution of $[Rh(COD)(\mu\text{-}Cl)]_2$ is added.

Introduction

A new tool for aqueous biphasic catalysis, which consists of stable aqueous dispersions of core-crosslinked micelles (CCMs) containing a core-anchored molecular catalyst, has been developed in one of our labs.[1-7] These micelles are unimolecular core-shell star polymers with a hydrophobic core and a hydrophilic shell (Figure 1a) and can be assembled in a straightforward two- or three-step one-pot convergent synthesis by RAFT polymerization[8-10] in water, which uses the polymerization-induced self-assembly (PISA) strategy,[11-13] to yield stable aqueous dispersions of the polymer particles (latex). The hydrophobic core, where catalysis takes place, ensures a suitable environment for the catalytic act under "homogeneous" conditions after swelling with an organic solvent (which may be the substrate itself), whereas the hydrophilic shell ensures confinement of the micelles in the aqueous phase, allowing facile catalyst recovery by decantation at the end of the reaction. Thus, each polymer particle acts in catalysis as an individual nanoreactor. The reactants, initially present in the organic bulk phase, migrate to the nanoreactor core through the hydrophilic shell and the products migrate in the opposite direction, to accumulate in the bulk organic phase for recovery. These migrations may introduce mass transfer limitations, but we have proven them to be minor for batch reactions with reasonably high stirring rates (*e.g.* 1200 rpm) and relatively low catalyst loadings.[2, 6]

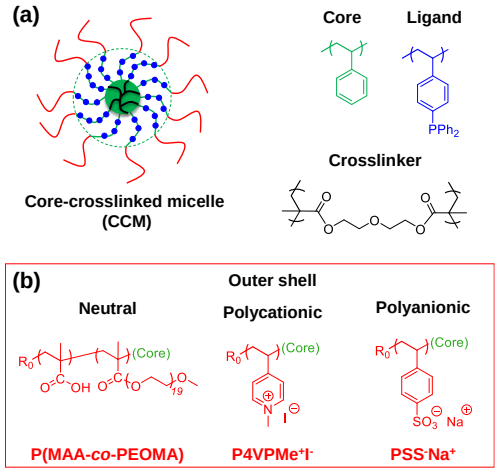

Figure 1. CCM topology (a) and chemical nature of neutral and charged chains in the hydrophilic shell (b).

[a] Dipartimento di Chimica, Università degli studi di Bari "Aldo Moro", via Orabona, 4, 70125 Bari Italy
[b] DICATECh, Politecnico di Bari, via Orabona, 4, 70125 Bari Italy
[c] CNRS, LCC (Laboratoire de Chimie de Coordination), UPS, INPT, Université de Toulouse, 205 route de Narbonne, F-31077 Toulouse, Cedex 4, France.
[d] Institut Universitaire de France, 1, rue Descartes, 75231 Paris (France).

Electronic Supplementary Information (ESI) available: Additional spectra and DFT results; table of energies and Cartesian coordinates for all optimized geometries (10 pages). See DOI: 10.1039/x0xx00000x

The 1st-generation CCMs have a neutral shell composed of statistical copolymer chains of methacrylic acid (MAA) and poly(ethylene oxide) methyl ether methacrylate (PEOMA), namely R_0-[$MAA_{0.5}$-*co*-$PEOMA_{0.5}$]$_{30}$-(hydrophobic core), where R_0 (-C(Me)(CN)CH_2CH_2COOH) is the initiating radical (Figure 1b). These chains contain carboxylic acid functionalities that render the shell pH-sensitive. Given the pK_a range of the carboxylic functions in PMMA (5.2–8.8),[14-16] the latex generates only a limited amount of anionic carboxylate functions by self-dissociation in neutral water (the natural pH of the as-synthesized latex is *ca.* 3.5[1]), while the shell can be fully deprotonated only at high pH. The Rh^I pre-catalyst was anchored onto the core-linked triphenylphosphine (TPP) ligands by diffusion of either [Rh-acac)$(CO)_2$] (acac = acetylacetonate) or [Rh(COD)(μ-Cl)]$_2$ (COD = 1,5-cyclooctadiene), which required prior core swelling with a good solvent (*e.g.* toluene or dichloromethane). Subsequent equilibration of the latex with the corresponding organic solution of the pre-catalyst precursor led to migration of the metal complex through the hydrophilic shell and to its anchoring by ligand exchange. Loading with [Rh(acac)$(CO)_2$], an olefin hydroformylation pre-catalyst, leads to core-anchored [Rh(acac)(CO)(TPP)],[1-4, 6, 7, 17] whereas loading with [Rh(COD)(μ-Cl)]$_2$, a hydrogenation pre-catalyst, leads to core-anchored [RhCl(COD)(TPP)].[18]

During this pre-catalyst loading process, it was noted that an efficient transfer of the [Rh(COD)(μ-Cl)]$_2$ complex only takes place when using toluene solutions,[18, 19] whereas attempts to load the pre-catalyst from a dichloromethane solution led to coagulation of the dispersed polymer micelles. On the other hand, the [Rh(acac)$(CO)_2$] complex could be transferred to the CCM cores equally efficiently from solutions in either solvent.[1-3, 5, 6, 17] A tentative interpretation of this phenomenon is based on the higher dichloromethane solvent permittivity, which may favour exchange reactions between the Cl ligand in the [Rh(COD)(μ-Cl)]$_2$ pre-catalyst and the shell carboxylic acid functions, anchoring neutral [Rh_2(COD)$_2$(O_2C-polymer)$_2$] or anionic [Rh(COD)(O_2C-polymer)$_2$]$^-$ complexes on the shell. Therefore, coagulation might result from coupling of different micelles *via* these Rh complexes as crosslinks. For the [Rh(acac)$(CO)_2$] precursor, on the other hand, the stronger donor power and chelating nature of the acetylacetonate ligand renders it resistant to exchange. This proposition is indirectly supported by the absence of any coagulation when loading 2nd-generation CCMs that have polycationic shells of poly(*N*-methyl-4-vinylpyridinium iodide) chains (P4NVPMe$^+$I$^-$, Figure 1b) with [Rh(COD)(μ-Cl)]$_2$ from dichloromethane solutions.[20] On the other hand, coagulation again takes place when loading 3rd-generation equivalent polymers with polyanionic shells of poly(sodium styrene sulfonate) chains (PSS$^-$Na$^+$, Figure 1b), even when using the lower-permittivity toluene medium.[21] In the latter case, molecular control experiments gave evidence in favour of [Rh(COD)]$^+$-sulfonate interactions, which are enhanced by the proximity of sulfonate groups (chelate effect), thus presumably leading to shell-anchored, crosslinking [Rh_2(COD)$_2$(O_3S-polymer)$_2$] or [Rh(COD)(O_3S-polymer)$_2$]$^-$ moieties.[21]

A number of complexes with the [Rh^I(alkene)$_2$(O_2CR)] stoichiometry, all of them adopting a dinuclear structure with two bridging carboxylates (Scheme 1A), have been described in the literature (alkene = C_2H_4[22] or dialkene = COD[23-32] or norbornadiene (NBD)[28, 33, 34]; R = various alkyl and aryl substituents). Mononuclear derivatives with a monodentate carboxylate and additional neutral ligands have also been described,[35-37] but no anionic bis(carboxylate) derivative (B) appears to be documented. On the other hand, the addition of an additional anionic ligand to other bridged Rh^I dimers is known to produce anionic bis-ligand adducts, *e.g.* [Rh(COD)Cl_2]$^-$.[38-43] In the present contribution, we report investigations revealing the equilibrium formation of a molecular [Rh(COD)$(OAc)_2$]$^-$ complex from the interaction between [Rh(COD)(μ-OAc)]$_2$ and the acetate ion, as well as spectroscopic evidence for an interaction between either [Rh(COD)(μ-Cl)]$_2$ or [Rh(COD)(μ-OAc)]$_2$ with a linear polymer that reproduces the chemical environment of the 1st-generation CCM particles, thus allowing to rationalize the above-mentioned coagulation phenomenon.

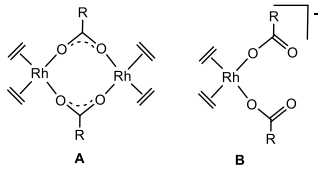

Scheme 1. Structures of known [Rh^I(alkene)$_2$(O_2CR)]$_2$ complexes (**A**) and of the putative anionic carboxylate adducts, [Rh^I(alkene)$_2$(O_2CR)$_2$]$^-$ (**B**).

Results and Discussion

(a) Spectroscopic characterization of [Rh(COD)(μ-OAc)]$_2$

Compound [Rh(COD)(μ-OAc)]$_2$ has been known since 1965[44] and its di-μ-acetato-bridged dinuclear structure has been established by X-ray diffraction,[32] but its spectroscopic characterization has so far been limited to a low-resolution ^{1}H NMR spectrum in $CDCl_3$ at room temperature,[45] while the ^{13}C NMR spectrum does not appear to be reported. Inspection of the ^{1}H NMR spectrum in CD_2Cl_2 at room temperature clearly indicates dynamic behaviour (Figure S1). The complex features three rather broad resonances (relative intensities 4:4:4) for the COD ligand at δ 4.08, 2.70 and 1.81, the latter being split into a doublet ($J_{H,Rh}$ = 7.5 Hz) by Rh coupling, and a sharper resonance for the acetate Me protons (intensity 3) at δ 1.70. This suggests a dynamic D_{2h} symmetry for the dinuclear molecule (local C_{2v} symmetry for the COD ligand), whereas the published structure[32] has only an overall C_{2v} symmetry with local C_s symmetry for the COD ligands. In principle, the inversion of the C_{2v} geometry can be achieved either *via* a dinuclear intermediate or *via* formation of two monomer molecules (Scheme 2). The same dynamic phenomenon with inversion of a dimeric C_{2v} structure has already been reported for dinuclear Rh^I complexes with amido[46] or phosphinato bridging ligands.[47]

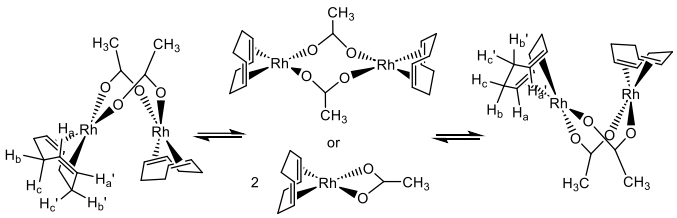

Scheme 2. Interpretation of the dynamic behavior of the [Rh(COD)(μ-OAc)]$_2$ compound.

The results of a variable-temperature ^{1}H NMR investigation are shown in Figure 2. The acetate Me singlet resonance is nearly temperature-invariant, whereas the two sp^3 CH protons resonances of the COD ligand, attributed to H_b, H_b', H_c and H_c', split into two equal intensity components at T ≤ 273 K (δ 2.75 and 2.49; δ 1.78 and 1.69). Further splitting becomes visible at 243 K for these resonances, more clearly for the two lower-frequency ones, but also hinted for the other two. The higher-frequency COD resonance, assigned to the sp^2 CH protons H_a and H_a', remains a single (albeit broad) signal down to 213 K, indicating a lower chemical shift difference, or accidental degeneracy, for the two inequivalent protons H_a and H_a'.

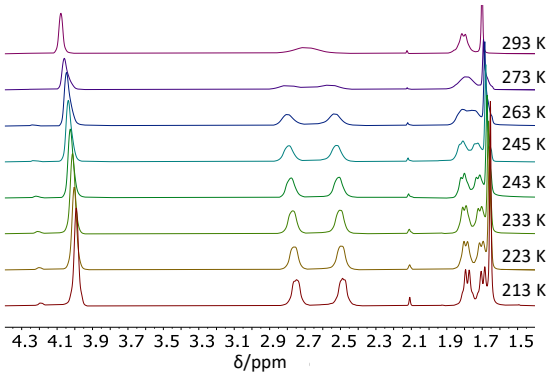

Figure 2. VT ^{1}H NMR spectra of [Rh(COD)(μ-OAc)]$_2$ in CD_2Cl_2.

A ^{1}H COSY spectrum recorded at 253 K (Figure S2) shows no correlation between the decoalesced resonances, consistent with the structural assignments of the resonances (the H_b/H_b' and H_c/H_c' pairs do not mutually couple), but reveals correlation within the H_a/H_b/H_c and H_a'/H_b'/H_c' sets. A ^{1}H-EXSY spectrum recorded at 233 K (Figure S3) confirms the exchange between the two protons at δ 2.75 and 2.49.

The previously unreported ^{13}C{^{1}H} NMR spectrum (Figure 3) of [Rh(COD)(μ-OAc)]$_2$ also presents broadened resonances at room temperature. Cooling to 223 K yields the expected number of resonances for the C_{2v} dimeric structure. The low-temperature spectrum exhibits two singlet resonances at δ 32.0 and 31.3 (collapsed into a broad resonance at δ 31.6 at 298 K), assigned to the sp^3-COD atoms, two doublet resonances at δ 81.5 (d, $J_{C,Rh}$ = 14.0 Hz) and 74.5 (d, $J_{C,Rh}$ = 13.6 Hz), still decoalesced as two very broad resonances at 298 K, assigned to the COD sp^2-C atoms, a singlet at δ 24.9 for the acetate Me group and a singlet at δ 183.0 for the carboxylate C nucleus. The latter two signals remain sharp at room temperature. The ^{1}H-^{13}C HMQC spectrum (Figure S4) at 223 K confirms the correlations of the COD sp^3-C resonances at δ 32.0 and 31.3 with those of the H_b, H_b', H_c and H_c' protons, and of the COD *sp*^{2} C resonances at δ 81.5 and 74.5 with that of the overlapping H_a and H_a' protons.

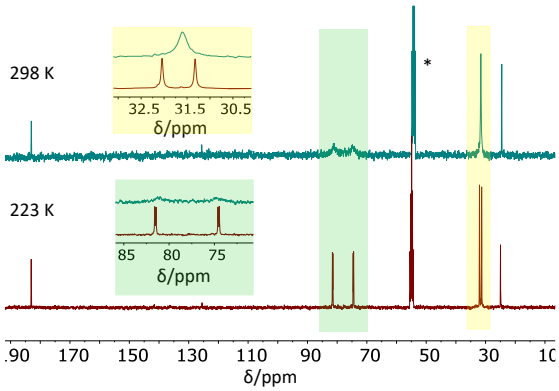

Figure 3. ^{13}C{^{1}H} NMR spectra of [Rh(COD)(μ-OAc)]$_2$ in CD_2Cl_2 at room temperature and at -50 °C. The starred resonance is due to the solvent.

(b) Acetate ion addition to [Rh(COD)(μ-OAc)]$_2$

The interaction between [Rh(COD)(μ-OAc)]$_2$ and excess acetate anion was investigated by NMR spectroscopy in CD_2Cl_2 at -60 °C in the presence of increasing amounts of [PPN]$^+$OAc$^-$. The salient results of the ^{1}H NMR investigation are shown in Figure 4. The resonances of the [Rh(COD)(μ-OAc)]$_2$ complex (red circles) decrease in intensity, while new resonances (green squares) appear and grow as the amount of added [PPN]$^+$OAc$^-$ increases, attesting to the transformation of [Rh(COD)(μ-OAc)]$_2$ into a new species. However, the addition is equilibrated (Scheme 3), because the [Rh(COD)(μ-OAc)]$_2$ resonances do not completely disappear after the addition of > 1 equivalent of [PPN]$^+$OAc$^-$ per Rh atom, while the resonance of the free OAc$^-$ reagent is visible even for solutions containing a substoichiometric amount (*e.g.* 0.44 equiv in Figure 4c).

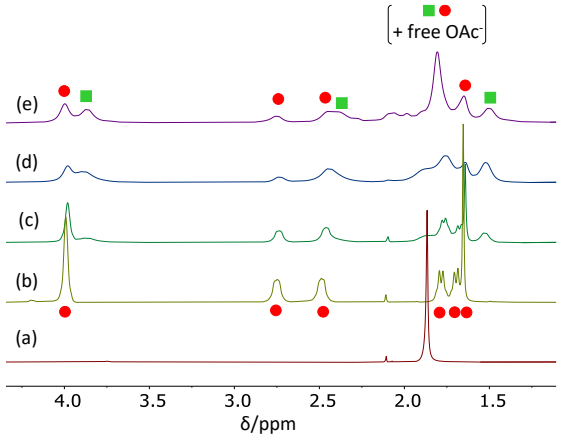

Figure 4. ^{1}H NMR spectra, recorded in CD_2Cl_2 at 213 K, for solutions of [PPN]$^+$OAc$^-$ (a) and [Rh(COD)(μ-OAc)]$_2$ (30 mg, 0.11 mmol of Rh) in the presence of various amounts of [PPN]$^+$OAc$^-$ (equivalents per Rh atom in parentheses): (b) no added salt; (c) 29 mg (0.049 mmol, 0.44 equiv); (d) 59 mg (0.099 mmmol, 0.90 equiv); (e) 81 mg (0.136 mmol, 1.23 equiv). The resonances marked with a red circle belong to [Rh(COD)(μ-OAc)]$_2$ and those marked with a green square to the new species formed in the reaction.

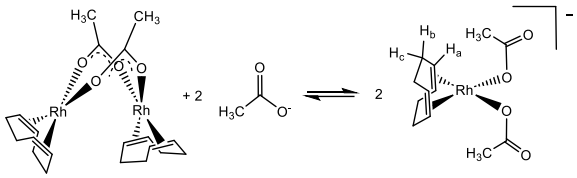

Scheme 3. Equilibrated acetate addition to $[Rh(COD)(\mu\text{-}OAc)]_2$.

The new species generated by the equilibrated reaction is characterized by four broad resonances, three of which are clearly visible at δ 3.87, 2.37 (shoulder of the $[Rh(COD)(\mu\text{-}OAc)]_2$ resonance at δ 2.46) and 1.52, while a fourth resonance can be guessed to overlap with the neutral dimer upper-field sp^3 CH_2 resonances in the δ 1.8-1.6 region. This pattern is consistent with high symmetry for the COD ligand and with formation of a mononuclear $[Rh(COD)(OAc)_2]^-$ ion, for which a C_{2v}-symmetric environment is expected. The observation of separate resonances for the new adduct, for the residual dimer, and for the excess free acetate indicates slow ligand exchange on the NMR timescale at 223 K.

Further information was obtained from a variable temperature study of the solution with the largest $[PPN]^+OAc^-$ excess (Figure 5). As the temperature was increased, the resonances of the new species and those of the residual $[Rh(COD)(\mu\text{-}OAc)]_2$ precursor coalesced, indicating that these two species rapidly exchange on the NMR timescale at the higher temperatures. The three coalesced resonances observed in the room temperature spectrum at δ 3.96, 2.50 and 1.62 have the same intensity, leading to their assignment to the COD ligand resonances. Therefore, the more intense resonance at δ 1.80 belongs to the acetate Me group, showing rapid exchange not only for the acetate ligands in the two Rh complexes with each other, but also with the excess of free acetate ion.

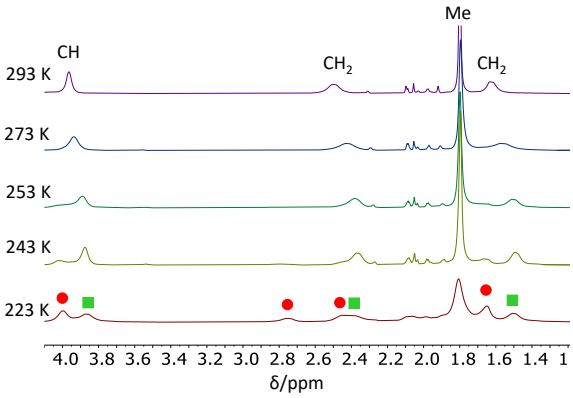

Figure 5. ^1H NMR spectra of the solution containing $[Rh(COD)(\mu\text{-}OAc)]_2$ (30 mg) and $[PPN]^+OAc^-$ (81 mg, 1.23 equiv per Rh atom) in CD_2Cl_2 at different temperatures.

The corresponding $^{13}C\{^1H\}$ NMR investigation confirms the above conclusion, but also reveals additional interesting features. The spectra of the $[PPN]^+OAc^-$ addition experiments at 213 K are shown in Figure 6. As in the above-described ^1H investigation, the $[Rh(COD)(\mu\text{-}OAc)]_2$ resonances do not completely disappear in the presence of a $[PPN]^+OAc^-$ excess (Figure 6e). However, the acetate resonances of the $[Rh(COD)(OAc)_2]^-$ and free acetate ion are coalesced in both Me (δ 24.8) and COO (δ 177.7) regions. The acetate resonance of the neutral dimer complex, on the other hand, remains distinct (as observed most notably after the second addition, Figure 6d). The COD resonances of the two Rh species also remain distinct. This suggests that acetate exchange on the $[Rh(COD)(OAc)_2]^-$ complex does not involve the neutral complex and is faster than the dimer/anionic monomer exchange. In addition, the two COD resonances of $[Rh(COD)(OAc)_2]^-$, observed at δ 77.8 (sp^2 CH) and δ 31.2 (sp^3 CH_2) are broad, particularly the lower-field one (δ 76.6). This cannot be due to exchange with the neutral dimer, since the resonances of the neutral dimer remain sharp, nor to exchange with free acetate. It is possible that this phenomenon is related to a rotational barrier for the two acetate ligands in $[Rh(COD)(OAc)_2]^-$, which should also desymmetrize the COD resonances in the unattained slow rotational regime.

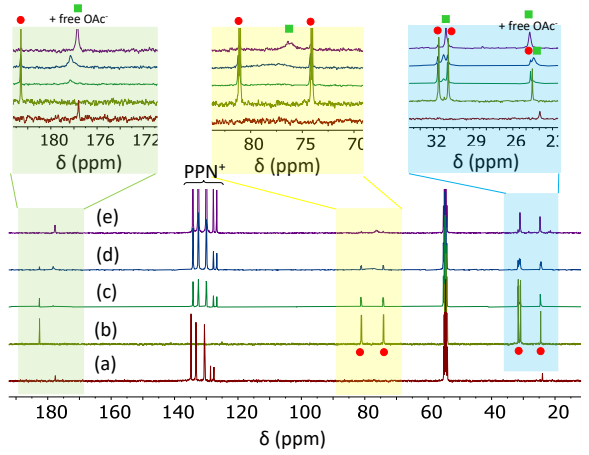

Figure 6. $^{13}C\{^1H\}$ NMR spectra, recorded in CD_2Cl_2 at 213 K, for solutions of $[PPN]^+OAc^-$ (a) and $[Rh(COD)(\mu\text{-}OAc)]_2$ (30 mg, 0.11 mmol of Rh) in the presence of various amounts of $[PPN]^+OAc^-$ (equivalents per Rh atom in parentheses): (b) no added salt; (c) 29 mg (0.049 mmol, 0.44 equiv); (d) 59 mg (0.99 mmmol, 0.90 equiv); (e) 81 mg (0.136 mmol, 1.23 equiv). The resonances marked with a red circle belong to $[Rh(COD)(\mu\text{-}OAc)]_2$ and those marked with a green square to the new species formed in the reaction.

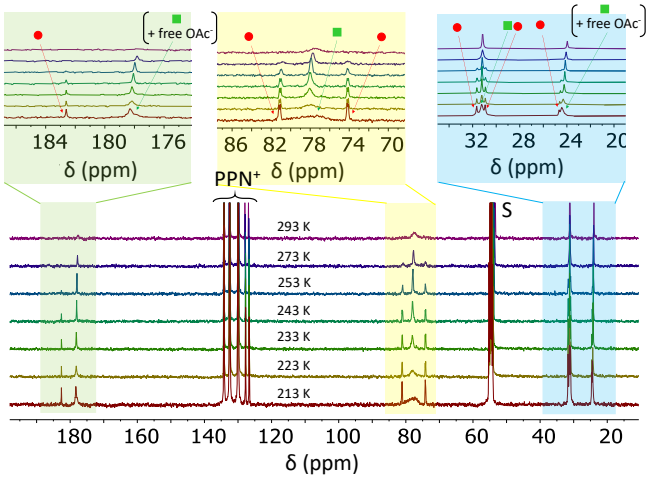

Figure 7. $^{13}C\{^1H\}$ NMR spectra of the solution containing $[Rh(COD)(\mu\text{-}OAc)]_2$ (30 mg) and $[PPN]^+OAc^-$ (59 mg, 0.90 equiv per Rh atom) in CD_2Cl_2 at different temperatures.

A variable temperature $^{13}C\{^1H\}$ NMR study, carried out after the second $[PPN]^+OAc^-$ addition where both neutral dimer and mononuclear anion are clearly visible (Figure 7), confirms that the $[Rh(COD)(\mu\text{-}OAc)]_2/[Rh(COD)(OAc)_2]^-$ exchange is activated only at the higher temperatures, while the $[Rh(COD)(OAc)_2]^-/OAc^-$ exchange is rapid at 213 K.

(c) DFT calculations

Further insights into the observed equilibria and exchange reactions were sought by DFT calculations. The energy values are reported as standard Gibbs energies in a dichloromethane solution (1 M, 298 K). Using the experimentally observed X-ray structure of $[Rh(COD)(\mu\text{-}OAc)]_2$ as guess geometry, the calculations yielded a very similar optimized geometry (comparison of observed and calculated bonding parameters in Table S1). A putative mononuclear complex with a bidentate chelating acetate ligand is computed as less stable: the rearrangement of one dimer molecules to yield two mononuclear complexes requires 10.3 kcal mol^{-1} per Rh atom. The addition of two acetate ions to the dimer to yield two $[Rh(COD)(OAc)_2]^-$ complexes, on the other hand, is exergonic, releasing 8.8 kcal mol^{-1} per Rh atom (Figure 8). This result qualitatively agrees with the spontaneous formation of the anionic complex upon treatment of $[Rh(COD)(\mu\text{-}OAc)]_2$ with acetate ions. However, the energy change is a bit too high for an equilibrated reaction. This discrepancy may be attributed, in addition to the computational error, to a possible role of the dichloromethane solvent in a preferential stabilization of the free acetate ion, *via* specific C-H···O interactions. It is indeed known that the C-H bond of dichloromethane is sufficiently polarized to engage in H-bonding with strong proton acceptors.[48, 49] Thus, the stronger electron density on the O atoms of free acetate, relative to those of the coordinated acetates in $[Rh(COD)(OAc)_2]^-$, may render the acetate coordination less favourable. Indeed, repeating the calculations in the presence of just one explicitly included CH_2Cl_2 slightly reduces the energy gain from –8.8 to –7.8 kcal mol^{-1}. The optimized geometries exhibit the expected C-H···O interactions for both free acetate and $[Rh(COD)(OAc)_2]^-$, with a shorter H···O with the free acetate ion (SI, Figure S5).

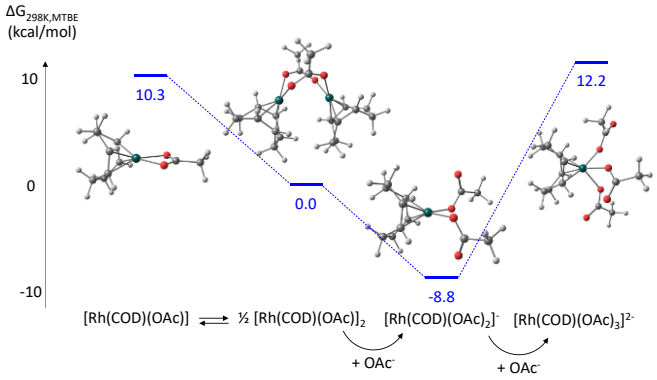

Figure 8. Gibbs energy profile for the $[Rh(COD)(\mu\text{-}OAc)]_2$ dimer/monomer conversion, for the reaction with acetate ions, and for the further acetate addition to $[Rh(COD)(OAc)_2]^-$.

Addition of yet another acetate ion to $[Rh(COD)(OAc)_2]^-$, yielding the 5-coordinate 18-electron triacetate dianion, $[Rh(COD)(OAc)_3]^{2-}$, raises the energy of the system by 21 kcal mol^{-1}, which is more than the energy cost of acetate dissociation to yield the mononuclear complex [Rh(COD)(OAc)] with a chelated acetate (19.1 kcal mol^{-1}). The calculations thus suggest that the preferred acetate exchange pathway in $[Rh(COD)(OAc)_2]^-$ is dissociative. If this is true, however, the mononuclear [Rh(COD)(OAc)] intermediate must add a new acetate ligand faster than dimerizing, since the dimer/anion exchange is slower.

(d) Acetate ligand exchange

The polymer coagulation phenomenon described in the Introduction was further addressed by experiments aimed at determining the aptitude of complexes $[Rh(COD)(\mu\text{-}Cl)]_2$ and $[Rh(COD)(\mu\text{-}OAc)]_2$, dissolved in either dichloromethane or toluene, to be transferred to an aqueous phase under three different conditions: (*i*) pure water; (*ii*) aqueous solution of sodium acetate; (*iii*) aqueous solution of the macroRAFT agent $R_0\text{-}[MAA_{0.5}\text{-}co\text{-}PEOMA_{0.5}]_{30}\text{-}SC(S)SnPr$, which is an intermediate of the neutral-shell nanoreactor synthesis (see Introduction). This short-chain polymer contains a 50:50 mixture of methacrylic acid and poly(ethylene oxide) methyl ether methacrylate (PEOMA) as co-monomers, the latter one ensuring its water solubility.

The two complexes do not have any affinity for water: their solution in both organic solvents (yellow) do not visually show any transfer of coloration to a water layer after extensive shaking and decantation (Figure S6a). The same behaviour was witnessed when mixing the organic solution of the Rh complexes with an aqueous solution of sodium acetate (Figure S6b), indicating that the formation of the anionic complex is not sufficiently favoured under these biphasic conditions. On the other hand, using an aqueous solution of the macroRAFT agent resulted in evident transfer of the Rh complex to the aqueous phase, even though the transfer was not complete (some yellow coloration also remained in the organic phase, see Figure 9).

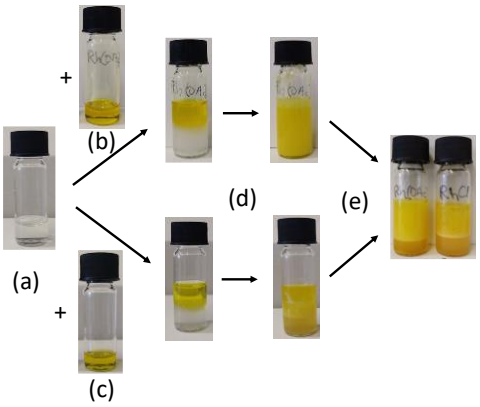

Figure 9. Exposure of toluene solutions of $[Rh(COD)(\mu\text{-}OAc)]_2$ (above) and $[Rh(COD)(\mu\text{-}Cl)]_2$ (below) to an aqueous solutions of $R_0\text{-}[MAA_{0.5}\text{-}co\text{-}PEOMA_{0.5}]_{30}\text{-}SC(S)SnPr$. (a) Aqueous solution of the macroRAFT agent (90 mmol of COOH functions); (b) $[Rh(COD)(\mu\text{-}OAc)]_2$ (18 mmol of Rh); (c) $[Rh(COD)(\mu\text{-}Cl)]_2$ (18 mmol of Rh); (d) vigorous stirring followed by standing for 5 min; (e) additional vigorous stirring (20 min) followed by standing for 30 min.

The occurrence of an interaction between [Rh(COD)(μ-OAc)]$_2$ and the macroRAFT agent was independently verified by an ^{1}H NMR investigation in the compatibilizing THF-d_8 solvent, Figure 10. The room temperature spectrum of [Rh(COD)(μ-OAc)]$_2$ (Figure 10a) is quite similar to that recorded at the same temperature in CD_2Cl_2, with broad resonances at δ 4.03 for the exchanging sp^2 CH protons and at δ 2.54 and 1.78 for the exchanging sp^3 CH protons. Figure 10b shows the spectrum of the polymer, the most prominent resonances of which are those of the PEO CH_2 protons at δ 3.60, overlapping with one of the two THF-d_8 residual resonances, and a much weaker resonance for the PEO chain-end OCH_3 protons at δ 3.30. The resonances of the polymer backbone protons (methacrylate in-chain CH and CH_2 and side-chain CH_3) are much broader and visible only at great magnification, because the chain is much less solvated, *i.e.* each polymer chain is self-organized as single-chain nanoparticles with a less solvated polymer backbone core and well-solvated, hence more mobile PEO-based shells. This result is consistent with a previously published ^{1}H NMR investigation of the 1st-generation CCM, demonstrating that the hydrocarbon skeleton of the outer-shell [$MAA_{0.5}$-*co*-$PEOMA_{0.5}$]$_{30}$ chains is not solvated by water and is located at the core-shell hydrophobic-hydrophilic interface.[5] The resonances of the R_0 and trithiocarbonate chain-ends are also unobserved, because of their small amount, but probably also because they are embedded within the unsolvated core of the self-organized single-chain particles. Upon combination of the two solutions (molar COOH/Rh ratio = 4:1), the spectrum (Figure 10c) no longer shows the resonances of the [Rh(COD)(μ-OAc)]$_2$ compound, but reveals new sharp resonance at δ 1.90, which belongs to free acetic acid. This assignment was confirmed by spiking the solution with additional CH_3COOH (Figure 10d). The COD resonances of [Rh(COD)(μ-OAc)]$_2$ have disappeared because the Rh complex is incorporated within the less mobile, unsolvated nanoparticle core by the carboxylate exchange.

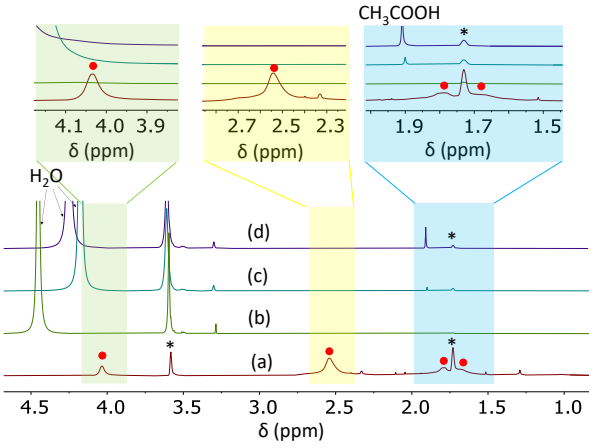

Figure 10. ^{1}H NMR spectra, recorded at room temperature in THF-d_8, of: (a) [Rh(COD)(μ-OAc)]$_2$; (b) the macroRAFT agent R_0-[$MAA_{0.5}$-*co*-$PEOMA_{0.5}$]$_{30}$-SC(S)S*n*Pr (R_0 = -C(Me)(CN)CH_2CH_2COOH); (c) a mixture of macroRAFT agent and [Rh(COD)(μ-OAc)]$_2$ (MAA/Rh = 4); (d) same as (c), after spiking with CH_3COOH. The starred resonances are due to the residual solvent protons.

All the above evidence indicates that, although an aqueous solution of the acetate ion is unable to replace chloride in [Rh(COD)(μ-Cl)]$_2$ when this is dissolved in an immiscible organic solvent, the exchange occurs with undissociated carboxylic acids in an hydrophobic environment (toluene, dichloro-methane) or in a compatibilizing medium (THF). Thus, when the organic solution of [Rh(COD)(μ-Cl)]$_2$ physically crosses the CCM neutral shell of the water-dispersed 1st-generation CCMs, the methacrylic acid functions of the [$MAA_{0.5}$-*co*-$PEOMA_{0.5}$]$_{30}$ chains come into contact with the Rh complex and fix the Rh complex on the CCM hydrophilic shell. Consequently, [Rh(COD)(μ-Cl)]$_2$ and the methacrylic acid functions meet in a homogeneous phase, rather than at the water/organic interphase, and can react with each other. The [Rh(COD)(μ-Cl)]$_2$ complex is then anchored onto the CCM shell as [Rh(COD)(μ-methacylate)]$_2$. Under these conditions, the formation of anionic [Rh(COD)(μ-methacylate)$_2$]$^-$ complexes is unlikely because the natural pH of the latex is acidic and only a tiny fraction of the MMA monomers is deprotonated. Thus, the anchored complex retains its dinuclear structure, which is however sufficient to provide particle coupling and coagulation, because the two methacrylates ligands may be provided by either the same CCM particle (either the same or two different $MAA_{0.5}$-*co*-$PEOMA_{0.5}$]$_{30}$ chains) or by the chains of two different particles.
As mentioned in the introduction, the [Rh(COD)(μ-Cl)]$_2$ complex could be loaded into the 1st-generation CCM core when using a toluene solution, whereas coagulation was observed when using dichloromethane. This difference may be related to the faster proton transfer from methacrylic acid to eventually release HCl. Thus, crossing the CCM shell and coordinating to the core TPP functions prevails in toluene, whereas the chloride/carboxylate exchange prevails in dichloromethane.

Experimental section

Compounds [Rh(COD)(μ-OAc)]$_2$,[50, 51] [PPN]$^+$OAc$^-$,[52] and the water-soluble R_0-[$MAA_{0.5}$-*co*-$PEOMA_{0.5}$]$_{30}$-SC(S)S*n*Pr polymer chains[1] were prepared according to the literature methods. [PPN]$^+$OAc$^-$ was crystallised from chloroform/ethyl acetate. NMR spectra were recorded with a Bruker Avance 400 spectrometer (400 MHz for ^{1}H); chemical shifts are reported in ppm referenced to $SiMe_4$ (^{1}H, ^{13}C) and 85% H_3PO_4 (^{31}P). The signal assignments were made based on a multinuclear NMR analysis of [Rh(COD)(μ-OAc)]$_2$ including, besides 1D spectra, ^{1}H-^{13}C HMQC, ^{1}H COSY and ^{1}H NOESY experiments. The FT-IR spectrum was recorded on a Jasco FT/IR 4200 spectrophotometer (ATR in the range 4000–400 cm^{-1}).
[Rh(COD)(μ-OAc)]$_2$: δ_H(CD_2Cl_2, 213 K): 1.65 (6 H, s, CH_3), 1.69 (4 H, d, $J_{H,H}$ = 8.4 Hz, H_c'), 1.78 (4 H, d, $^1J_{H,H}$ = 8.4 Hz, H_c), 2.49 (4 H, broad, H_b'), 2.75 (4 H, broad, H_b), 3.99 (8 H, broad, H_a+ H_a'). δ_C(CD_2Cl_2, 298 K): 24.9 (s, CH_3), 31.3. (s, *C*-H_c), 32.0 (s, *C*-H_b), 74.5 (d, $J_{C,Rh}$ = 13.6 Hz, *C*-H_a'), 81.5 (d, $J_{C,Rh}$ = 14.0 Hz, *C*-H_a), 183.0 (COO). See spectra in Figures 2-7 and S1-4.
[PPN]$^+$OAc$^-$: δ_H(CD_2Cl_2, 298 K): 1.87 (3 H, s, CH_3), from 7.36 to 7.81 (30 H, m, Ph); δ_C(CD_2Cl_2, 298 K): 23.3 (CH_3), 127.4 (C_6H_5, d, $^1J_{H,P}$ = 108 Hz, C_{ipso}), 129.9 (C_6H_5, m, C_{ortho}), 132.5 (C_6H_5, m, C_{meta}), 134.1 (C_6H_5, s, C_{para}), 176.9 (COO); δ_P(CD_2Cl_2, 298 K): 21.0 (s). IR:

ν_{max}(ATR)/cm^{-1} 3056w, 1567m (OAc), 1386s, 1113s, 722s, 690s, 667m, 524vs, 500s, 451m. See spectra in Figures S7-9. The IR spectrum is shown in Figure S10.

Computational details. The calculations were carried out using the Gaussian16 suite of programs.[53] The geometry optimizations were performed without any symmetry constraint using the B3LYP functional.[54-56] The basis set comprised the SDD functions, with and SDD ECP and an f polarization function (α = 1.350)[57] and the 6-311G(d,p) basis functions for all other atoms. The effects of dispersion forces (Grimme's D3 empirical method[58]) and solvation effects (in dichloromethane, using the SMD approach[59]) were included during the optimization. The ZPVE, PV, and TS corrections at 298 K were obtained with Gaussian16 from the solution of the nuclear equation using the standard ideal gas and harmonic approximations at T = 298.15 K, which also verified the nature of all optimized geometries as local minima. A correction of 1.95 kcal/mol was applied to all G values to change the standard state from the gas phase (1 atm) to solution (1 M).[60]

Conclusions

The present investigation was inspired by the observation of polymer coagulation upon addition of [Rh(COD)(μ-Cl)]$_2$/dichloromethane to a stable latex of core-crosslinked micelles (CCM) with a methacrylate acid-containing hydrophilic outer shell. The investigations have established that while both [Rh(COD)(μ-Cl)]$_2$ and [Rh(COD)(μ-OAc)]$_2$ do not interact with aqueous acetate ions, an exchange process with release of acetic acid from [Rh(COD)(μ-OAc)]$_2$ and presumably of HCl from [Rh(COD)(μ-Cl)]$_2$ occurs when the compounds are exposed to a water-soluble polymer chain containing methacrylic acid monomers. The study has also revealed the formation of equilibrium amounts of the previously unreported [Rh(COD)(OAc)$_2$]$^-$ complex, which has been fully characterized in solution, in the presence of free acetate. Notably, this anionic complex undergoes rapid exchange with the [Rh(COD)(μ-OAc)]$_2$ precursor and an even more rapid exchange with free acetate. The presence of this equilibrium, however, is unlikely to be the main reason of the observed CCM coagulation. The formation of the [Rh(COD)(μ-methacrylate)]$_2$ complex linked to the CCM shell chains is sufficient to account for this phenomenon.

Author Contributions

AMF and VP: investigation, writing – review and editing. CF: supervision, formal analysis, writing - review and editing. EM, funding acquisition, writing - review and editing. PM: supervision, formal analysis, writing - review and editing. RP: conceptualisation, investigation (DFT calculations), writing – original draft.

Conflicts of interest

There are no conflicts to declare.

Acknowledgements

We gratefully acknowledged the Agence Nationale de la Recherche (project BIPHASNANOCAT, grant No. 11-BS07-025-01) for funding. We thank Politecnico di Bari for support of an internship of A.M.F. at the LCC Toulouse. RP is grateful to the CALMIP mesocenter of the University of Toulouse for the allocation of computational resources.

Notes and references

1. X. Zhang, A. F. Cardozo, S. Chen, W. Zhang, C. Julcour, M. Lansalot, J.-F. Blanco, F. Gayet, H. Delmas, B. Charleux, E. Manoury, F. D'Agosto and R. Poli, *Chem. Eur. J.*, 2014, **20**, 15505–15517.
2. A. F. Cardozo, C. Julcour, L. Barthe, J.-F. Blanco, S. Chen, F. Gayet, E. Manoury, X. Zhang, M. Lansalot, B. Charleux, F. D'Agosto, R. Poli and H. Delmas, *J. Catal.*, 2015, **324**, 1-8.
3. S. Chen, A. F. Cardozo, C. Julcour, J.-F. Blanco, L. Barthe, F. Gayet, B. Charleux, M. Lansalot, F. D'Agosto, H. Delmas, E. Manoury and R. Poli, *Polymer*, 2015, **72**, 327-335.
4. R. Poli, S. Chen, X. Zhang, A. Cardozo, M. Lansalot, F. D'Agosto, B. Charleux, E. Manoury, F. Gayet, C. Julcour, J.-F. Blanco, L. Barthe and H. Delmas, *ACS Symp. Ser.*, 2015, **1188**, 203-220.
5. S. Chen, F. Gayet, E. Manoury, A. Joumaa, M. Lansalot, F. D'Agosto and R. Poli, *Chem. Eur. J.*, 2016, **22**, 6302 – 6313.
6. E. Lobry, A. F. Cardozo, L. Barthe, J.-F. Blanco, H. Delmas, S. Chen, F. Gayet, X. Zhang, M. Lansalot, F. D'Agosto, R. Poli, E. Manoury and C. Julcour, *J. Catal.* , 2016, **342**, 164-172.
7. E. Manoury, F. Gayet, F. D'Agosto, M. Lansalot, H. Delmas, C. Julcour, J.-F. Blanco, L. Barthe and R. Poli, in *Effects of Nanoconfinement on Catalysis*, ed. R. Poli, Springer, New York, 2017, pp. 147-172.
8. J. Chiefari, Y. K. Chong, F. Ercole, J. Krstina, J. Jeffery, T. P. T. Le, R. T. A. Mayadunne, G. F. Meijs, C. L. Moad, G. Moad, E. Rizzardo and S. H. Thang, *Macromolecules*, 1998, **31**, 5559-5562.
9. G. Moad, E. Rizzardo and S. H. Thang, *Austr. J. Chem.*, 2005, **58**, 379-410.
10. C. Barner-Kowollik, ed., *Handbook of RAFT Polymerization*, Wiley-VCH, Weinheim, 2008.
11. N. J. W. Penfold, J. Yeow, C. Boyer and S. P. Armes, *ACS Macro Lett.*, 2019, **8**, 1029-1054.
12. M. Lansalot and J. Rieger, *Macromol. Rapid Comm.*, 2019, **40**.
13. F. D'Agosto, J. Rieger and M. Lansalot, *Angew. Chem. Int. Ed.*, 2020, **59**, 8368-8392.
14. J. Zhang and N. A. Peppas, *Macromolecules*, 2000, **33**, 102-107.
15. T. Ikawa, K. Abe, K. Honda and E. Tsuchida, *J. Polym. Sci., Polym. Chem.*, 1975, **13**, 1505-1514.
16. H. Dong, H. Du and X. Qian, *J. Phys. Chem. B*, 2009, **113**, 12857-12859.
17. A. Joumaa, F. Gayet, E. J. Garcia-Suarez, J. Himmelstrup, A. Riisager, R. Poli and E. Manoury, *Polymers*, 2020, **12**, 1107/1101-1118.
18. A. Joumaa, S. Chen, S. Vincendeau, F. Gayet, R. Poli and E. Manoury, *Mol. Cat.*, 2017, **438**, 267-271.
19. S. Chen, E. Manoury, F. Gayet and R. Poli, *Polymers*, 2016, **8**, 26/21-18.

20. H. Wang, L. Vendrame, C. Fliedel, S. Chen, F. Gayet, F. D'Agosto, M. Lansalot, E. Manoury and R. Poli, *Chem. Eur. J.*, 2021, **27**, 5205–5214.
21. H. Wang, C. J. Abou-Fayssal, C. Fliedel, E. Manoury and R. Poli, *Polymers*, 2022, **14**, 4937.
22. H. Werner, S. Poelsma, M. E. Schneider, B. Windmuller and D. Barth, *Chem. Ber.*, 1996, **129**, 647-652.
23. A. M. Trzeciak, J. J. Ziolkowski, T. Lis and A. Borowski, *Polyhedron*, 1985, **4**, 1677-1681.
24. E. Mieczynska, A. M. Trzeciak, J. J. Ziolkowski and T. Lis, *Polyhedron*, 1994, **13**, 655-658.
25. R. Fornika, E. Dinjus, H. Gorls and W. Leitner, *J. Organomet. Chem.*, 1996, **511**, 145-155.
26. S. M. Tetrick, F. S. Tham and A. R. Cutler, *J. Am. Chem. Soc.*, 1997, **119**, 6193-6194.
27. F. A. Cotton, E. V. Dikarev and M. A. Petrukhina, *J. Chem. Soc., Dalton Trans.*, 2000, DOI: 10.1039/b006894m, 4241-4243.
28. J. Zednik, J. Sedlacek, J. Svoboda, J. Vohlidal, D. Bondarev and I. Cisarova, *Collection of Czechoslovak Chemical Communications*, 2008, **73**, 1205-1221.
29. C. Pariya, Y. S. Marcos, Y. X. Zhang, F. R. Fronczek and A. W. Maverick, *Organometallics*, 2008, **27**, 4318-4324.
30. W. M. Alley, C. W. Girard, S. Ozkar and R. G. Finke, *Inorg. Chem.*, 2009, **48**, 1114-1121.
31. S. P. Wei, J. Pedroni, A. Meissner, A. Lumbroso, H. J. Drexler, D. Heller and B. Breit, *Chem. Eur. J.*, 2013, **19**, 12067-12076.
32. C. M. Filloux and T. Rovis, *J. Am. Chem. Soc.*, 2015, **137**, 508-517.
33. W. R. Cullen, S. J. Rettig and E. B. Wickenheiser, *Canadian Journal of Chemistry*, 1994, **72**, 1294-1301.
34. B. I. Azbel, N. F. Goldshleger, M. L. Khidekel, V. I. Sokol and M. A. Poraikoshits, *J. Mol. Catal.*, 1987, **40**, 57-63.
35. F. J. Lahoz, A. Martin, M. A. Esteruelas, E. Sola, J. L. Serrano and L. A. Oro, *Organometallics*, 1991, **10**, 1794-1799.
36. N. Imlinger, K. Wurst and M. R. Buchmeiser, *Monatsh. Chem.*, 2005, **136**, 47-57.
37. G. Choi, H. Tsurugi and K. Mashima, *J. Am. Chem. Soc.*, 2013, **135**, 13149-13161.
38. G. Vasapollo, A. Sacco, C. F. Nobile, M. A. Pellinghelli and M. Lanfranchi, *J. Organomet. Chem.*, 1986, **312**, 249-262.
39. N. Stylianides, A. A. Danopoulos and N. Tsoureas, *J. Organomet. Chem.*, 2005, **690**, 5948-5958.
40. L. Dahlenburg, H. Treffert, C. Farr, F. W. Heinemann and A. Zahl, *Eur. J. Inorg. Chem.*, 2007, DOI: 10.1002/ejic.200601215, 1738-1751.
41. M. Delferro, D. Cauzzi, R. Pattacini, M. Tegoni, C. Graiff and A. Tiripicchio, *Eur. J. Inorg. Chem.*, 2008, DOI: 10.1002/ejic.200800075, 2302-2312.
42. M. V. Jimenez, J. J. Perez-Torrente, M. I. Bartolome, V. Gierz, F. J. Lahoz and L. A. Oro, *Organometallics*, 2008, **27**, 224-234.
43. H. Ben-Daat, G. B. Hall, T. L. Groy and R. J. Trovitch, *Eur. J. Inorg. Chem.*, 2013, **2013**, 4430-4442.
44. S. D. Robinson and B. L. Shaw, *J. Chem. Soc.*, 1965, DOI: 10.1039/jr9650004997, 4997-5001.
45. A. A. H. Van der Zeijden, G. Van Koten, R. A. Nordemann, B. Kojic-Prodic and A. L. Spek, *Organometallics*, 1988, **7**, 1957.
46. C. Tejel, M. A. Ciriano, M. Bordonaba, J. A. Lopez, F. J. Lahoz and L. A. Oro, *Chem. Eur. J.*, 2002, **8**, 3128-3138.
47. A. Iturmendi, P. J. S. Miguel, S. A. Popoola, A. A. Al-Saadi, M. Iglesias and L. A. Oro, *Dalton Trans.*, 2016, **45**, 16955-16965.
48. E. S. Kryachko and T. Zeegers-Huyskens, *J. Phys. Chem. A*, 2001, **105**, 7118-7125.
49. P. A. Dub, N. V. Belkova, O. A. Filippov, J.-C. Daran, L. M. Epstein, A. Lledós, E. S. Shubina and R. Poli, *Chem. Eur. J.*, 2010, **16**, 189-201.
50. J. Chatt and L. M. Venanzi, *J. Chem. Soc.*, 1957, DOI: 10.1039/jr9570004735, 4735-4741.
51. W. S. Sheldrick and B. Guenther, *J. Organomet. Chem.*, 1989, **375**, 233-243.
52. N. Y. Kozitsyna, A. A. Bukharkina, M. V. Martens, M. N. Vargaftik and I. I. Moiseev, *J. Organomet. Chem.*, 2001, **636**, 69-75.
53. M. J. Frisch, G. W. Trucks, H. B. Schlegel, G. E. Scuseria, M. A. Robb, J. R. Cheeseman, G. Scalmani, V. Barone, G. A. Petersson, H. Nakatsuji, X. Li, M. Caricato, A. V. Marenich, J. Bloino, B. G. Janesko, R. Gomperts, B. Mennucci, H. P. Hratchian, J. V. Ortiz, A. F. Izmaylov, J. L. Sonnenberg, D. Williams-Young, F. Ding, F. Lipparini, F. Egidi, J. Goings, B. Peng, A. Petrone, T. Henderson, D. Ranasinghe, V. G. Zakrzewski, J. Gao, N. Rega, G. Zheng, W. Liang, M. Hada, M. Ehara, K. Toyota, R. Fukuda, J. Hasegawa, M. Ishida, T. Nakajima, Y. Honda, O. Kitao, H. Nakai, T. Vreven, K. Throssell, J. A. Montgomery Jr., J. E. Peralta, F. Ogliaro, M. J. Bearpark, J. J. Heyd, E. N. Brothers, K. N. Kudin, V. N. Staroverov, T. A. Keith, R. Kobayashi, J. Normand, K. Raghavachari, A. P. Rendell, J. C. Burant, S. S. Iyengar, J. Tomasi, M. Cossi, J. M. Millam, M. Klene, C. Adamo, R. Cammi, J. W. Ochterski, R. L. Martin, K. Morokuma, O. Farkas, J. B. Foresman and D. J. Fox, *Gaussian 16, Revision B.01*, Gaussian, Inc., Wallingford CT, 2016.
54. C. T. Lee, W. T. Yang and R. G. Parr, *Phys. Rev. B*, 1988, **37**, 785-789.
55. B. Miehlich, A. Savin, H. Stoll and H. Preuss, *Chem. Phys. Lett.*, 1989, **157**, 200-206.
56. A. D. Becke, *J. Chem. Phys.*, 1993, **98**, 5648-5652.
57. A. W. Ehlers, M. Böhme, S. Dapprich, A. Gobbi, A. Hoellwarth, V. Jonas, K. F. Koehler, R. Stegmann, A. Veldkamp and G. Frenking, *Chem. Phys. Lett.*, 1993, **208**, 111-114.
58. S. Grimme, J. Antony, S. Ehrlich and H. Krieg, *J. Chem. Phys.*, 2010, **132**, 154104.
59. A. V. Marenich, C. J. Cramer and D. G. Truhlar, *J. Phys. Chem. B*, 2009, **113**, 6378-6396.
60. V. S. Bryantsev, M. S. Diallo and W. A. Goddard, III, *J. Phys. Chem. B*, 2008, **112**, 9709-9719.